In-vitro and *In-silico* Investigations of Recent and Traditional Antifungal Agents as Inhibitors of Fungal Chitin Synthesis

Samy Selim [a,*] Mohammed Ibrahim Alghonaim [b,*] Sulaiman A. Alsalamah [b] Shaza N. Alkhatib,[c] Sahar Abdulaziz Alshareef [c] Mohammed S. Almuhayawi,[d] Hattan S. Gattan,[e,f] and Mohammed H. Alruhaili [d,f]

** Corresponding author: sabdulsalam@ju.edu.sa (S.S.); mialghonaim@imamu.edu.sa (M.I.A.)*

DOI: 10.15376/biores.21.3.7317-7330

GRAPHICAL ABSTRACT

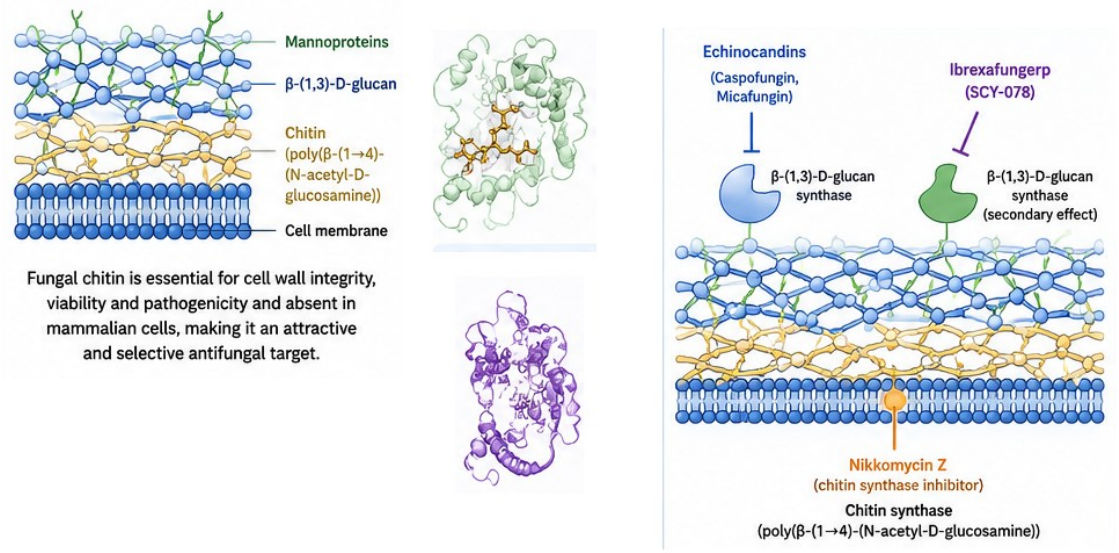

In-vitro and *In-silico* Investigations of Recent and Traditional Antifungal Agents as Inhibitors of Fungal Chitin Synthesis

Samy Selim [a,*] Mohammed Ibrahim Alghonaim [b,*] Sulaiman A. Alsalamah [b] Shaza N. Alkhatib,[c] Sahar Abdulaziz Alshareef [c] Mohammed S. Almuhayawi,[d] Hattan S. Gattan,[e,f] and Mohammed H. Alruhaili [d,f]

Invasive fungal infections demand novel approaches targeting cell wall components, particularly poly(β)-(1→4)-(N-acetyl-D-glucosamine) (chitin) and β-glucan. This study evaluated Caspofungin, Micafungin, Ibrexafungerp, and Nikkomycin Z against *Aspergillus fumigatus* and *Candida albicans*. Moreover, the binding affinity and interaction profiles of Caspofungin, Micafungin, Ibrexafungerp (SCY-078), and Nikkomycin Z against two crystallographic targets: Calcineurin A from *A. fumigatus* (PDB ID: 6TZ7) and poly(β)-(1→4)-(N-acetyl-D-glucosamine) synthase 2 from *C. albicans* (PDB ID: 7STN), using Molecular Operating Environment (MOE) docking were evaluated. Micafungin showed highest monotherapy activity (21 ± 0.8 and 25 ± 0.9 mm), while Micafungin–Ibrexafungerp produced maximal inhibition (29 ± 1.0 and 28 ± 0.9 mm), indicating synergistic cell wall disruption and species-dependent variability. Docking scores revealed that Micafungin exhibited the strongest binding toward 6TZ7 (S = −10.96 kcal/mol) and 7STN (S = −13.82 kcal/mol). Nikkomycin Z demonstrated multiple hydrogen bonding interactions within the catalytic pocket of poly(β)-(1→4)-(N-acetyl-D-glucosamine) synthase 2, consistent with its known mechanism as a poly(β)-(1→4)-(N-acetyl-D-glucosamine) synthase inhibitor. These findings support differential binding behaviors of echinocandins, triterpenoid glucan synthase inhibitors, and poly(β)-(1→4)-(N-acetyl-D-glucosamine) synthase inhibitors toward key fungal enzymes and provide structural insight into their antifungal mechanisms.

DOI: 10.15376/biores.21.3.7317-7330

Keywords: poly(β)-(1→4)-(N-acetyl-D-glucosamine) targeting; Antifungal; Molecular docking; Aspergillus fumigatus; Candida albicans

Contact information: a: Department of Clinical Laboratory Sciences, College of Applied Medical Sciences, Jouf University, Sakaka, Saudi Arabia; b: Department of Biology, College of Science, Imam Mohammad Ibn Saud Islamic University (IMSIU), Riyadh 11623, Saudi Arabia; c: Department of Biological Sciences, Collage of Sciences and Arts Khulais, University of Jeddah, Jeddah, Saudi Arabia; d: Department of Clinical Microbiology and Immunology, Faculty of Medicine, King Abdulaziz University, Jeddah 21589, Saudi Arabia; e: Department of Medical Laboratory Technology, Faculty of Applied Medical Sciences, King Abdulaziz University, Jeddah 21589, Saudi Arabia; f: Special Infectious Agents Unit, King Fahad Medical Research Center, King AbdulAziz University, Jeddah, Saudi Arabia;

** Corresponding author: sabdulsalam@ju.edu.sa (S.S.); mialghonaim@imamu.edu.sa (M.I.A.)*

INTRODUCTION

The fungal cell wall is a vital and dynamic construction that plays a necessary role in maintaining cell integrity, shape, and survival. It primarily consists of β-(1,3)-D-glucan, poly(β)-(1→4)-(N-acetyl-D-glucosamine) (chitin), besides mannoproteins, making it an attractive target for antifungal drug development, as these ingredients are missing in animal cells. Among these, poly(β)-(1→4)-(N-acetyl-D-glucosamine) that plays a fundamental role in maintaining cell wall rigidity, integrity, and mechanical strength. It is essential for fungal viability, growth, hyphal elongation, septum formation, morphogenesis, and spore development.

In addition, poly(β)-(1→4)-(N-acetyl-D-glucosamine) contributes significantly to fungal adaptation under environmental and osmotic stress conditions by reinforcing the cell wall architecture and protecting fungal cells from mechanical damage and external stressors. Dynamic remodeling of poly(β)-(1→4)-(N-acetyl-D-glucosamine) within the cell wall is also crucial during fungal development, host interaction, and stress adaptation processes Hokken *et al.* 2019). Numerous studies have demonstrated that enzymes involved in the metabolism of poly(β)-(1→4)-(N-acetyl-D-glucosamine), including deacetylases and chitinases, participate in fungal pathogenicity, immune evasion, and cell wall restructuring during environmental challenges (Moussian 2019; Asif *et al.* 2020). Furthermore, oligomers derived from poly(β)-(1→4)-(N-acetyl-D-glucosamine) are involved in host–pathogen interactions and innate immune recognition mechanisms, highlighting their biological importance in fungal survival and pathogenicity (Chang *et al.* 2025). Because poly(β)-(1→4)-(N-acetyl-D-glucosamine) is absent in mammalian cells, its biosynthetic pathway represents an attractive and selective target for antifungal drug development. Inhibition of poly(β)-(1→4)-(N-acetyl-D-glucosamine) synthesis disrupts normal cell wall assembly, leading to impaired growth, abnormal morphology, weakened stress tolerance, and eventual fungal cell death (Liu *et al.* 2026).

Among microbial infections, fungi remain a serious agent for human infections causing high morbidity and mortality rate worldwide, particularly in cases suffering from immune-compromise problems (Kim *et al.* 2025). Among the most clinically significant fungal pathogens, *Aspergillus fumigatus* and *Candida albicans* are responsible for a wide range of invasive and superficial infections (Cedeño-Pinargote *et al.* 2025).

Echinocandins as antifungal agents, including caspofungin and micafungin, that inhibit the activity of β-(1,3)-D-glucan synthase, is accompanied by cell walls weakening and death of cells (Ramos *et al.* 2025). However, exposure to echinocandins has been associated with a compensatory increase in poly(β)-(1→4)-(N-acetyl-D-glucosamine) synthesis in some fungal species, which may contribute to minimized sensitivity or tolerance (Walker *et al.* 2008; Walker *et al.* 2015). These highlights the importance of directly targeting poly(β)-(1→4)-(N-acetyl-D-glucosamine) synthesis as a complementary or substitute antifungal strategy (Antachopoulos *et al*. 2008; Fuentefria *et al.* 2018).

Ibrexafungerp (SCY-078) is a recent orally bioavailable antifungal agent that also inhibits β-(1,3)-D-glucan synthase, but it joins to a different site than echinocandins, potentially overcoming some resistance mechanisms. On the other hand, Nikkomycin Z is a traditional antifungal compound that specifically inhibits poly(β)-(1→4)-(N-acetyl-D-glucosamine) synthase by acting as a competitive analog of UDP-N-acetylglucosamine,

directly blocking the synthesis of poly(β)-(1→4)-(N-acetyl-D-glucosamine) in the fungal cell wall (El Ayoubi *et al.* 2024).

Despite their distinct mechanisms of action, comparative studies evaluating the effects of caspofungin, micafungin, ibrexafungerp, and nikkomycin Z on growth of *A. fumigatus* and *C. albicans* remain limited (Kovács *et al.* 2019). Moreover, integrating *in vitro* antifungal susceptibility testing with *in silico* molecular docking and interaction analyses can provide valuable insights into drug-target binding, stability, and potential structure–activity relationships (Qanash *et al.* 2023a). Therefore, this study aims to investigate and compare the antifungal activity of caspofungin, micafungin, ibrexafungerp (SCY-078), and nikkomycin Z against *A. fumigatus* and *C. albicans* through combined *in vitro* and *in silico* approaches.

EXPERIMENTAL

Antifungal Activity Assay

The antifungal activity of caspofungin, micafungin, ibrexafungerp (SCY-078), and nikkomycin Z, individually and in combination, was evaluated against *Aspergillus fumigatus* and *Candida albicans* using the agar well diffusion method. Fungal strains were subcultured on Sabouraud Dextrose Agar (SDA) plates and incubated at 28 °C for 48 to 72 h. Fresh colonies were suspended in sterile saline solution and adjusted to a turbidity equivalent to 0.5 McFarland standard (approximately 1×10^6 CFU/mL for *C. albicans* and spores/mL for *A. fumigatus*). Sterile SDA plates were uniformly inoculated by swabbing the standardized fungal suspension over the agar surface. Wells (6 mm in diameter) were aseptically punched into the agar using a sterile cork borer. Each well was filled with a fixed volume (100 µL) of the test compound (single drug or drug combination). Plates were left at room temperature for 1.0 h to allow diffusion and then incubated at 28 °C for 48 h. After incubation, the diameter of the clear inhibition zone surrounding each well was measured in millimeters using a digital caliper.

Determination of Poly(β)-(1→4)-(N-acetyl-D-glucosamine) Content in Fungal Cells

The content of poly(β)-(1→4)-(N-acetyl-D-glucosamine) in fungal cells was determined by measuring the amount of glucosamine released following acid hydrolysis of the fungal cell wall (Chen and Johnson 1983). *Aspergillus fumigatus* and *Candida albicans* were cultured on Sabouraud Dextrose Broth (SDB) in the presence or absence of the tested antifungal treatments and incubated at 28 °C for 48 h under shaking conditions. Fungal biomass from *A. fumigatus* mycelia and *C. albicans* yeast cells was collected by centrifugation and washed twice with sterile distilled water. One g fresh fungal biomass was frozen in liquid nitrogen and thoroughly homogenized using a sterile mortar and pestle. The homogenized material was suspended in 2 mL deionized water and centrifuged at 13,000 ×g for 10 min at 4 °C to isolate the cell wall fraction. The resulting pellet was freeze-dried overnight. Dried cell wall samples (2 to 6 mg) were hydrolyzed with 1 mL of 6 M HCl at 100 °C for 4 h. After cooling to room temperature, 0.2 mL of the hydrolysate was mixed with 0.25 mL of 4% acetylacetone prepared in 1.25 M sodium carbonate solution and incubated at 90 °C for 1 h. After cooling, 2 mL ethanol were added with continuous

agitation until complete dissolution of the precipitate. Subsequently, 0.25 mL of Ehrlich's reagent [1.6 g N,N-dimethyl-p-aminobenzaldehyde dissolved in 60 mL ethanol:HCl (1:1, v/v)] was added for color development. The absorbance was recorded at 530 nm using a UV–Visible spectrophotometer (UV-1800, Shimadzu Corporation, Kyoto, Japan). The concentration of glucosamine released from fungal cell wall poly(β)-(1→4)-(N-acetyl-D-glucosamine) was calculated using a standard calibration curve prepared with known concentrations of glucosamine hydrochloride and expressed as µg glucosamine hydrochloride per mg dry cell wall weight.

Molecular Docking Analysis

The crystal structures of calcineurin A from *A. fumigatus* (6TZ7) and poly(β)-(1→4)-(N-acetyl-D-glucosamine) synthase 2 from *C. albicans* (7STN) were retrieved from the Protein Data Bank (http://www.rcsb.org). Protein structures were prepared using Molecular Operating Environment (MOE, Chemical Computing Group, Montreal, Canada).

Preparation steps included: Removal of co-crystallized ligands and water molecules, addition of hydrogen atoms, assignment of protonation states at physiological pH (7.4), and energy minimization using the MMFF94x force field until RMS gradient convergence. Dummy atoms were used to precisely characterize the active sites of both enzymes. Caspofungin, Micafungin, Ibrexafungerp (SCY-078), and Nikkomycin Z were constructed, and energy minimized using MMFF94x. Conformational searches were performed, and the lowest-energy conformers were used for docking.

Docking was performed in MOE using Placement: Triangle Matcher.
Scoring function: London dG (initial scoring).
Refinement: Forcefield refinement.
Final scoring: GBVI/WSA dG.

Five poses per ligand were generated, and the best-ranked pose based on S-score (kcal/mol) and interaction consistency was selected for analysis.

RESULTS AND DISCUSSION

Table 1 presents the inhibition zone diameters (mm, mean ± SD) of two fungal species, *A. fumigatus* and *C. albicans*, treated with traditional echinocandins (Caspofungin and Micafungin) and recently developed antifungal agents (Ibrexafungerp (SCY-078) and Nikkomycin Z). *Candida albicans* showed greater susceptibility than *A. fumigatus* to all tested monotherapies. Among the single agents, Micafungin exhibited the strongest antifungal activity against both fungi, producing inhibition zones of 21 ± 0.8 mm for *A. fumigatus* and 25 ± 0.9 mm for *C. albicans*. Caspofungin demonstrated moderate activity (17 ± 0.6 mm and 22 ± 0.7 mm, respectively). The newer agents, Ibrexafungerp and Nikkomycin Z, showed comparatively lower inhibition zones, particularly against *A. fumigatus*. The relatively small standard deviation values indicate good reproducibility of the assay. Combination therapy markedly improved antifungal efficacy compared with single-drug treatments (Table 2). The most pronounced effect was observed with the Micafungin + Ibrexafungerp combination, yielding inhibition zones of 29 ± 1.0 mm against *A. fumigatus* and 28 ± 0.9 mm against *C. albicans*. Similarly, Caspofungin combined with Ibrexafungerp or Nikkomycin Z proved increased inhibitory effects relative to

monotherapy. These findings suggest a potential synergistic interaction between echinocandins and the newer antifungal agents, leading to improved fungal growth suppression. Remarkably, *C. albicans* appeared more responsive than *A. fumigatus* across all single treatments, indicating species-dependent variability in susceptibility. The pairing of micafungin with ibrexafungerp produced the most pronounced inhibitory effect against both fungal strains, while other combinations also proved substantial enhancements compared to single-drug utilization. This amplified activity may suggest additive or synergistic interactions between agents targeting different components of the fungal cell wall, thereby strengthening growth suppression. Susceptibility to echinocandins varies among *Aspergillus* species, with *A. niger* being more sensitive to caspofungin than *A. fumigatus*, likely due to alterations in cell wall composition (Imhof *et al.*, 2003). Laboratory-generated *A. fumigatus* mutants further highlight mechanisms of reduced caspofungin sensitivity (Gardiner *et al.* 2005). Nikkomycin Z strongly improves the activity of echinocandins against *Candida* biofilms, producing multiple-fold reductions in MIC values for both *C. albicans* and *C. parapsilosis* when applied in combination (Kovács *et al.* 2019). These notes support the potential of combination therapies to improve antifungal efficacy and overcome reduced susceptibility.

Table 1. Inhibition (mm) of Fungi by Traditional and Recent Antifungal Drugs

Fungi	Caspofungin	Micafungin	Ibrexafungerp (SCY-078)	Nikkomycin Z
A. fumigatus	17 ± 0.6	21 ± 0.8	16 ± 0.5	15 ± 0.7
C. albicans	22 ± 0.7	25 ± 0.9	21 ± 0.6	19 ± 0.8

Table 2. Inhibition (mm) of Fungi by Combining Traditional and Recent Antifungal Drugs

Fungi	Caspofungin+ Ibrexafungerp (SCY-078)	Micafungin+ Ibrexafungerp (SCY-078)	Caspofungin+ Nikkomycin Z	Micafungin+ Nikkomycin Z
A. fumigatus	26 ± 0.9	29 ± 1.0	23 ± 0.7	25 ± 0.8
C. albicans	27 ± 0.8	28 ± 0.9	27 ± 0.7	28 ± 0.8

The determination of fungal cell wall poly(β)-(1→4)-(N-acetyl-D-glucosamine) content demonstrated that all tested antifungal compounds significantly reduced the major structural polysaccharide components of the fungal cell wall in both *A. fumigatus* and *C. albicans* compared with the untreated control. The untreated *A. fumigatus* cells exhibited a poly(β)-(1→4)-(N-acetyl-D-glucosamine) content of 82.4 µg glucosamine hydrochloride/ mg dry cell wall weight, whereas treatment with Nikkomycin Z reduced the value to 52.6 µg/mg. An even greater reduction was observed with combination therapies, particularly Micafungin + Nikkomycin Z, which decreased the content to 31.7 µg/mg. Similarly, in *C. albicans*, the untreated control showed 76.8 µg/mg, while the same combination reduced the level to 29.4 µg/mg (Table 3). These findings are consistent with the antifungal inhibition zones presented in Tables 1 and 2, where combination treatments exhibited stronger antifungal activity than single-drug treatments.

The marked reduction in fungal cell wall poly(β)-(1→4)-(N-acetyl-D-glucosamine) content correlated with the increased inhibition zones, suggesting that disruption of fungal cell wall biosynthesis contributes significantly to fungal growth suppression. Our results

were in agreement with previous study but on other fungi namely *Phytophthora infestans* and *Saprolegnia parasitica* (Guerriero *et al.* 2010). Measurement of fungal cell wall poly(β)-(1→4)-(N-acetyl-D-glucosamine) (glucosamine) content represents one of the important mechanistic approaches for confirming inhibition of fungal growth by the antifungal compounds (Santos *et al*. 2025; Xu *et al.* 2025). Reduction of glucosamine levels indicates impairment of fungal cell wall assembly and structural integrity, supporting the molecular docking findings that predicted strong interactions between the tested compounds and fungal cell wall biosynthetic targets.

Table 3. Effect of Antifungal Treatments on Cell Wall Poly(β)-(1→4)-(N-acetyl-D-glucosamine) Content Expressed as µg Glucosamine Hydrochloride/mg Dry Cell Wall Weight

Treatment	*A. fumigatus*	*C. albicans*
Control (without antifungal)	82.4 ± 2.1	76.8 ± 1.9
Caspofungin	69.5 ± 1.8	64.7 ± 1.7
Micafungin	66.2 ± 1.6	61.9 ± 1.5
Ibrexafungerp (SCY-078)	71.8 ± 1.9	67.3 ± 1.8
Nikkomycin Z	52.6 ± 1.4	49.8 ± 1.3
Caspofungin + Ibrexafungerp	48.9 ± 1.2	45.1 ± 1.1
Micafungin + Ibrexafungerp	44.3 ± 1.1	41.7 ± 1.0
Caspofungin + Nikkomycin Z	36.5 ± 0.9	33.8 ± 0.8
Micafungin + Nikkomycin Z	31.7 ± 0.8	29.4 ± 0.7

Molecular docking was employed in this study as a supportive *in silico* tool to predict the possible interactions between the tested antifungal compounds and key fungal target proteins. This approach helps to provide a mechanistic explanation for the observed antifungal effects by suggesting potential binding at enzymes involved in cell wall biosynthesis and cellular regulation as mentioned in numerous studies deals with other targets (Yahya *et al.* 2022; Al-Rajhi *et al.* 2023; Alsalamah *et al.* 2023; Qanash *et al.* 2023b; Al-Rajhi *et al.* 2025). Molecular docking analysis against the 6TZ7 target protein of *A. fumigatus* revealed favorable binding affinities for all tested antifungal compounds. Among the evaluated ligands, Micafungin demonstrated the strongest predicted binding affinity with an S-score of −10.96 kcal/mol, followed by Caspofungin (−9.07 kcal/mol), Ibrexafungerp (−7.33 kcal/mol), and Nikkomycin Z (−6.62 kcal/mol) (Table 4). Interaction profiling showed that Caspofungin formed multiple hydrogen bond interactions with GLN18, HIS337, and TYR339 residues within the active site. On the other hand, docking with 7STN (*C. albicans*) demonstrated that binding scores were −13.82, −12.34, −8.92, and −8.66 kcal/mol of Micafungin, Caspofungin, Ibrexafungerp, and Nikkomycin Z, respectively (Table 5). Micafungin exhibited hydrogen bonding with TYR339 in addition to π-interactions involving TRP340, which may contribute to its superior binding stability. Ibrexafungerp interacted through hydrogen bonding with GLN18 and π-interaction with TYR49, whereas Nikkomycin Z formed strong hydrogen bond interactions with GLU51 and TYR339, including a notable interaction energy of −3.3 kcal/mol with GLU51. Furthermore, RMSD_refine values ranging from 1.19 to 2.17 Å confirmed the stability and reliability of the predicted docking conformations (Table 6). Micafungin demonstrated the most favorable predicted binding. Key interactions indicated that Caspofungin formed hydrogen bonds with GLU321 and ASP856. Micafungin interacted with LYS440, ASN438,

and ILE857. Ibrexafungerp formed a hydrogen bond with LYS748. Nikkomycin Z established multiple hydrogen bonds, notably with TYR600 (−4.7 kcal/mol), ASP856, and ASN438, in addition to π-H interactions with LEU601 and ARG646 (Table 7). The extensive hydrogen bonding network of Nikkomycin Z within the catalytic region supports its known inhibitory function. Echinocandins (Caspofungin and Micafungin) are clinically established inhibitors of β-1,3-D-glucan synthase, disrupting fungal cell wall synthesis. Although calcineurin is not their primary molecular target, inhibition of calcineurin signaling has been associated with increased susceptibility to cell wall stress and antifungal agents (Steinbach *et al.* 2006). The strong docking scores of Micafungin toward 6TZ7 suggest potential secondary interactions that may contribute to stress pathway modulation. Ibrexafungerp (SCY-078) is a triterpenoid glucan synthase inhibitor structurally distinct from echinocandins but sharing the same enzymatic target (Davis *et al.* 2020). Its moderate docking scores toward both proteins are consistent with its specificity for glucan synthase rather than calcineurin or poly(β)-(1→4)-(N-acetyl-D-glucosamine) synthase. Nikkomycin Z is a competitive inhibitor of poly(β)-(1→4)-(N-acetyl-D-glucosamine) synthase, mimicking UDP-N-acetylglucosamine (Georgopapadakou and Tkacz 1995). The multiple hydrogen bonds observed with catalytic residues such as ASP856 and TYR600 in 7STN align with the established mechanism of poly(β)-(1→4)-(N-acetyl-D-glucosamine) synthase inhibition and support its selective activity against *Candida* species. poly(β)-(1→4)-(N-acetyl-D-glucosamine) synthase 2 is critical for septum formation and cell wall integrity in *C. albicans* (Brain *et al.* 2025). The superior binding scores of Micafungin and Caspofungin toward 7STN suggest possible structural complementarity within the catalytic pocket, although their primary clinical mechanism remains glucan synthase inhibition. Generally, the docking results align with established antifungal mechanisms while also highlighting potential secondary binding behaviors that could influence antifungal synergy.

Results of Docking with 6TZ7 (*A. fumigatus*) gave binding scores of −10.96, −9.07, −7.33, and −6.62 kcal/mol for Micafungin, Caspofungin, Ibrexafungerp, and Nikkomycin Z, respectively (Table 4). Micafungin exhibited the strongest predicted affinity. Interaction analysis revealed that Caspofungin formed H bonds with GLN18, HIS337, and TYR339. Micafungin showed H bonding with TYR339 and π-interactions with TRP340. Ibrexafungerp formed H bonding with GLN18 and π-interaction with TYR49. Nikkomycin Z established strong H bonding with GLU51 (−3.3 kcal/mol) and TYR339. RMSD_refined values ranged between 1.19 and 2.17 Å, indicating stable docking poses.

Table 4. Docking Scores and Energies for Caspofungin, Micafungin, Ibrexafungerp (SCY-078), and Nikkomycin Z with the Crystal Structure of *A. fumigatus* (PDB ID: 6TZ7)

Molecule	S	RMSD_ refine	E_conf	E_place	E_score 1	E_refine	E_score 2
Caspofungin	-9.07	1.39	-113.57	-49.23	-7.40	-54.62	-9.07
Micafungin	-10.96	1.85	-93.98	-53.31	-10.42	-67.68	-10.96
Ibrexafungerp	-7.33	2.17	-100.52	-47.40	-9.87	-41.82	-7.33
Nikkomycin Z	-6.62	1.20	-28.49	-73.20	-10.55	-34.11	-6.62

Although the present investigation provides useful insights into the antifungal activity and predicted molecular interactions of the tested compounds, certain limitations

should be noted. The proposed mechanism based on molecular docking was not confirmed by direct chitin synthase inhibition assays, and therefore it remains predictive. In addition, the measured reduction in fungal cell wall poly(β)-(1→4)-(N-acetyl-D-glucosamine) content reflects general cell wall alterations rather than specific enzymatic inhibition. Future work should include direct chitin synthase activity assays, or advanced structural techniques to validate the proposed mechanism.

Table 5. Docking Scores and Energies for Caspofungin, Micafungin, Ibrexafungerp (SCY-078), and Nikkomycin Z with Poly(β)-(1→4)-(N-acetyl-D-glucosamine) Synthase 2 from C. albicans (PDB ID: 7STN)

Molecule	S	RMSD_ refine	E_conf	E_place	E_score 1	E_refine	E_score 2
Caspofungin	-12.34	1.80	-143.05	-47.92	-3.46	-70.06	-12.34
Micafungin	-13.82	1.38	-109.72	-21.41	-1.32	-86.26	-13.82
Ibrexafungerp	-8.92	2.45	-131.93	-88.21	-9.29	-40.53	-8.92
Nikkomycin Z	-8.66	1.33	-9.29	-137.34	-11.40	-34.63	-8.66

Table 6. Interaction of Caspofungin, Micafungin, Ibrexafungerp (SCY-078), and Nikkomycin Z with the Crystal Structure of *A. fumigatus* (PDB ID: 6TZ7)

Molecule	Ligand	Receptor	Interaction	Distance	E (kcal/mol)
Caspofungin	O 1	O GLN 18 (A)	H-donor	3.03	-1.6
	N 24	O HIS 337 (A)	H-donor	3.07	-0.5
	O 4	N TYR 339 (A)	H-acceptor	2.80	-2.2
Micafungin	O 11	N TYR 339 (A)	H-acceptor	3.34	-0.6
	C 53	5-ring TRP 340 (A)	H-pi	4.43	-0.6
	C 53	6-ring TRP 340 (A)	H-pi	3.71	-0.8
Ibrexafungerp	N 8	N GLN 18 (A)	H-acceptor	3.23	-1.0
	C 53	6-ring TYR 49 (A)	H-pi	4.56	-0.5
Nikkomycin Z	O 2	O TYR 339 (A)	H-donor	2.76	-1.9
	O 4	OE1 GLU 51 (A)	H-donor	2.88	-3.3
	C 20	O TYR 339 (A)	H-donor	3.34	-1.0
	6-ring	CA ASP 346 (A)	pi-H	4.74	-0.5

Table 7. Interaction of Caspofungin, Micafungin, Ibrexafungerp (SCY-078), and Nikkomycin Z with Poly(β)-(1→4)-(N-acetyl-D-glucosamine) Synthase 2 from *C. albicans* (PDB ID: 7STN)

Mol	Ligand	Receptor	Interaction	Distance	E (kcal/mol)
Caspofungin	O 9	OE2 GLU 321 (A)	H-donor	3.05	-0.9
	O 12	OE1 GLU 321 (A)	H-donor	2.91	-0.7
	C 44	OD1 ASP 856 (A)	H-donor	3.48	-0.5
Micafungin	O 13	O ILE 857 (A)	H-donor	3.05	-0.7
	O 11	CE LYS 440 (A)	H-acceptor	3.23	-0.9
	O 14	ND2 ASN 438 (A)	H-acceptor	3.35	-0.6
	O 21	CA ALA 439 (A)	H-acceptor	3.37	-0.5
Ibrexafungerp	N 9	NZ LYS 748 (A)	H-acceptor	3.08	-2.2

Nikkomycin Z	O 3	OD1 ASP 856 (A)	H-donor	3.45	-0.5
	O 3	OD2 ASP 856 (A)	H-donor	3.03	-0.5
	O 4	O TYR 600 (A)	H-donor	2.75	-4.7
	C 32	O HIS 569 (A)	H-donor	3.25	-0.6
	C 34	O ASN 438 (A)	H-donor	3.36	-0.5
	O 5	N ILE 442 (A)	H-acceptor	3.30	-0.5
	6-ring	CA LEU 601 (A)	pi-H	3.81	-0.6
	6-ring	CA ARG 646 (A)	pi-H	3.87	-0.8

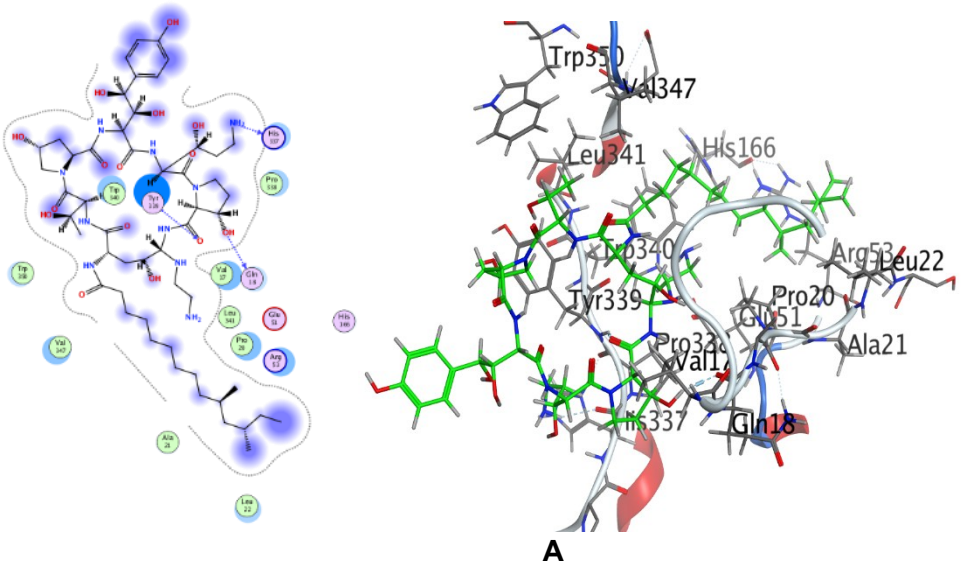

A

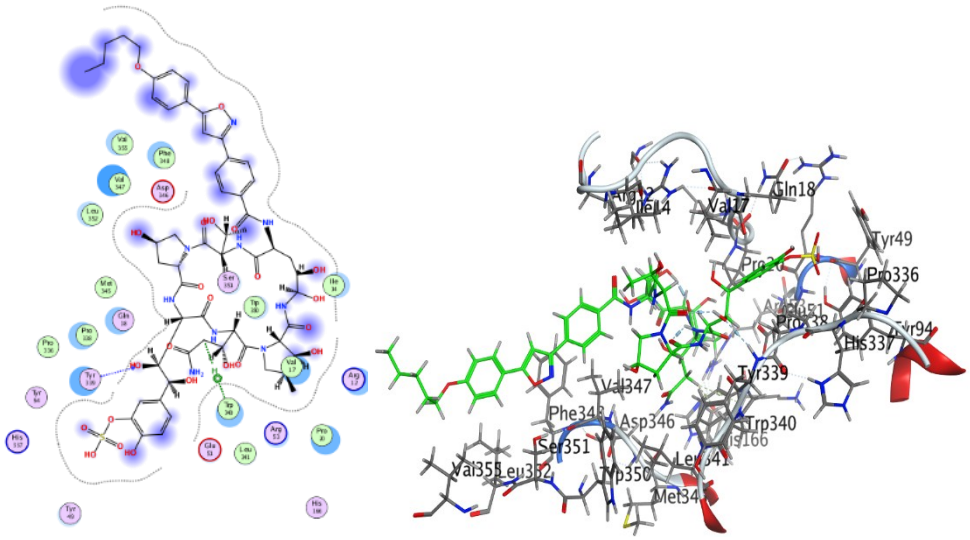

B

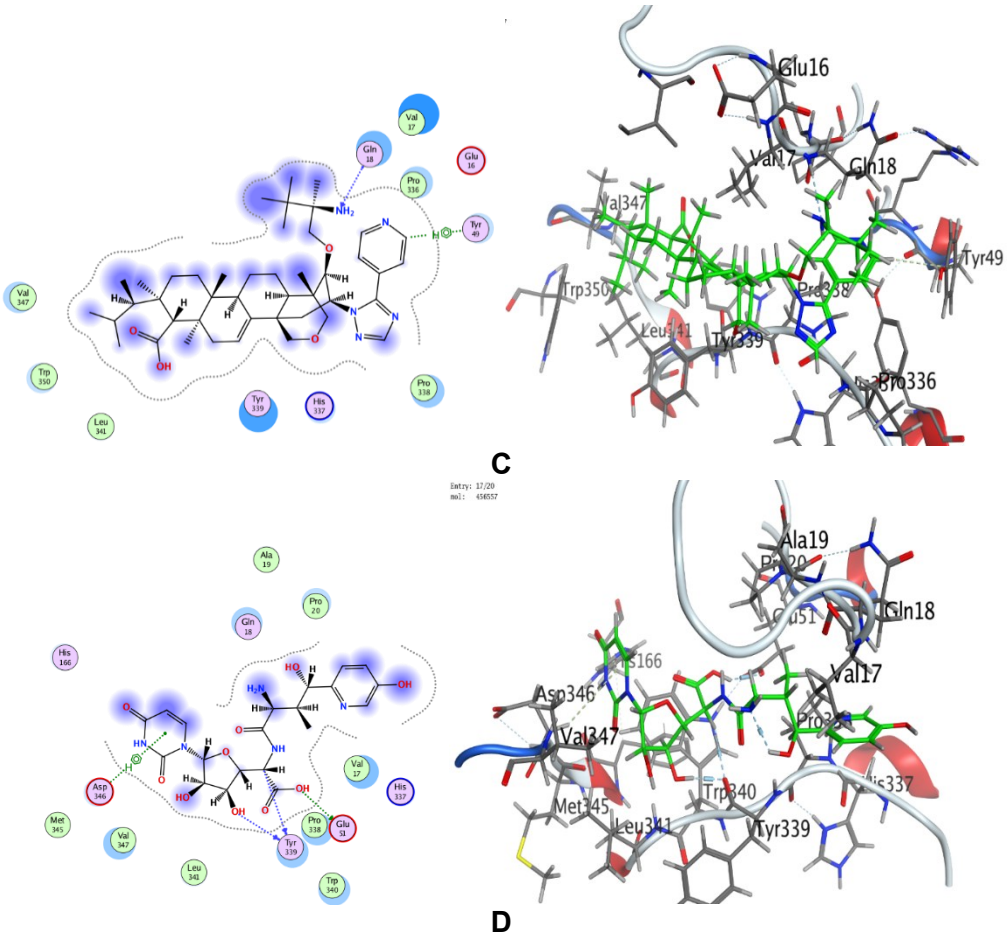

Fig. 1. 2D and 3D Diagrams show the interaction between Caspofungin (A), Micafungin (B), Ibrexafungerp (C), and Nikkomycin Z (D) with the active sites of *A. fumigatus* 6TZ7 protein

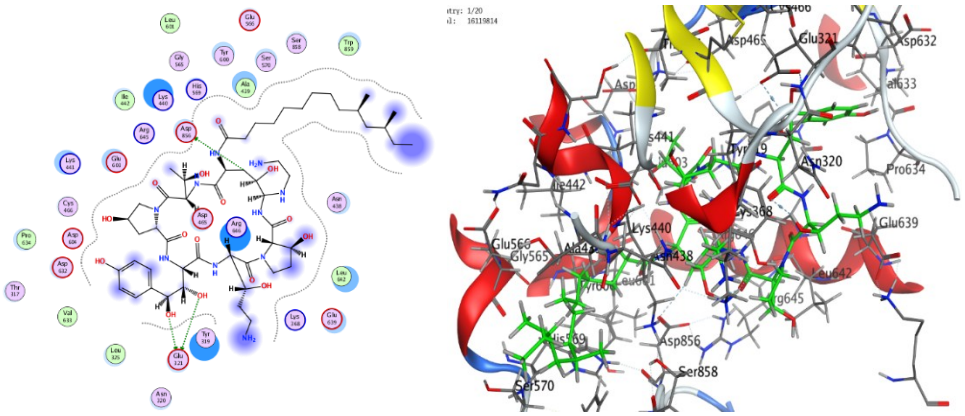

A

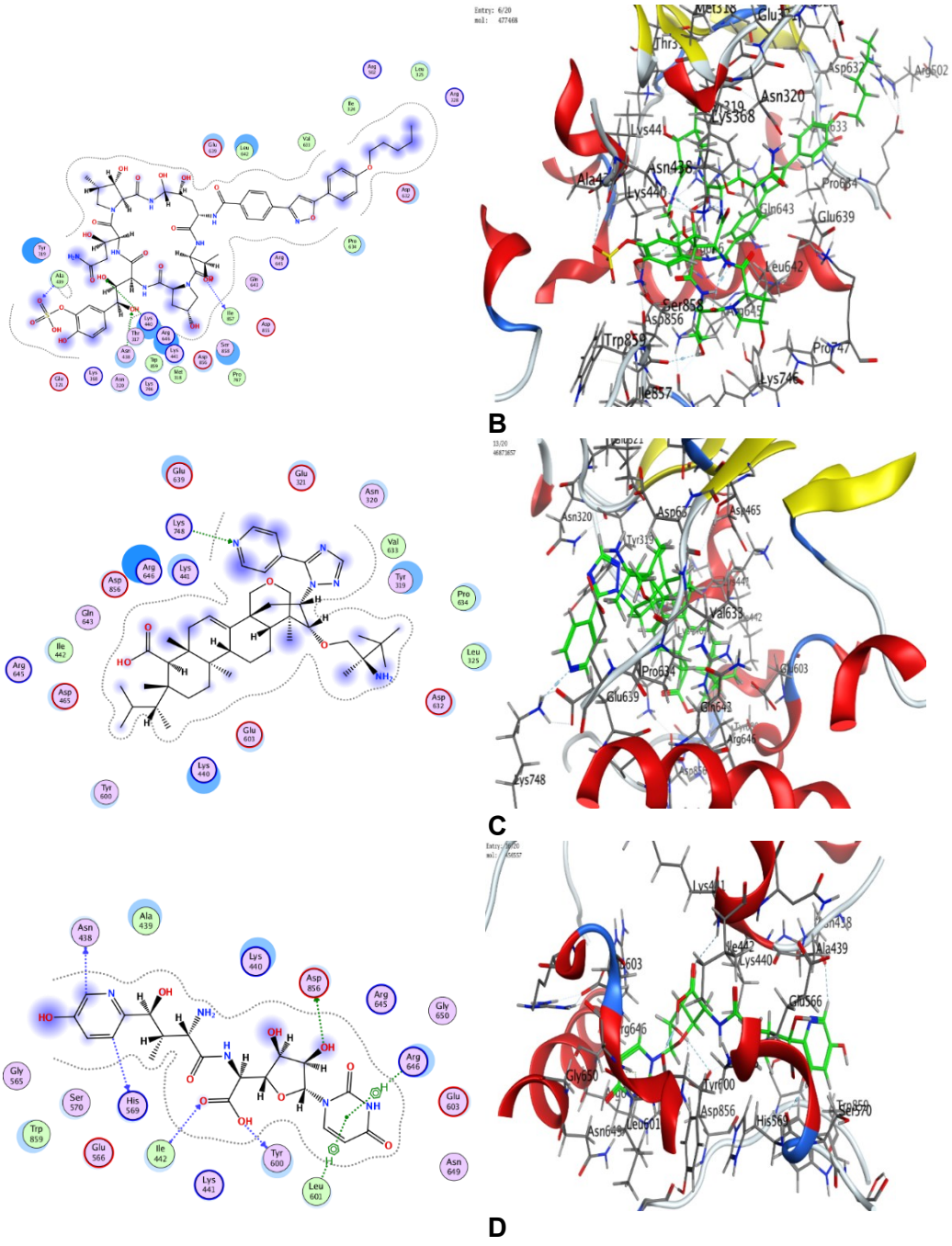

Fig. 2. 2D and 3D Diagrams show the interaction between Caspofungin (A), Micafungin (B), Ibrexafungerp (C), and Nikkomycin Z (D) with the active sites of *C. albicans* 7STN protein

CONCLUSIONS

1. Combined inhibition of major fungal cell wall biosynthetic pathways, including β-(1,3)-D-glucan synthesis and poly(β)-(1→4)-(N-acetyl-D-glucosamine) synthesis, significantly enhanced antifungal activity against *Aspergillus fumigatus* and *Candida*

albicans. The combination treatments produced larger inhibition zones than the individual drugs in Petri dish assays, particularly Micafungin + Ibrexafungerp and Micafungin + Nikkomycin Z, indicating synergistic disruption of fungal cell wall integrity and fungal growth suppression.

2. Molecular docking analysis demonstrated that Micafungin exhibited the strongest predicted binding affinity toward both calcineurin A of *Aspergillus fumigatus* (6TZ7) and poly(β)-(1→4)-(N-acetyl-D-glucosamine) synthase 2 of *Candida albicans* (7STN), suggesting superior interaction stability with key fungal targets. In contrast, Nikkomycin Z showed highly specific interactions within the catalytic region of poly(β)-(1→4)-(N-acetyl-D-glucosamine) synthase 2, supporting its role as a selective inhibitor of fungal cell wall poly(β)-(1→4)-(N-acetyl-D-glucosamine) biosynthesis. These computational findings were supported by the experimental reduction in fungal cell wall poly(β)-(1→4)-(N-acetyl-D-glucosamine) content and the enhanced antifungal activity observed in the combination treatments.
3. Micafungin showed the strongest predicted binding to both targets. Nikkomycin Z demonstrated specific and extensive interactions within the catalytic site of poly(β)-(1→4)-(N-acetyl-D-glucosamine) synthase 2, supporting its mechanism as a poly(β)-(1→4)-(N-acetyl-D-glucosamine) synthesis inhibitor. The findings provide structural insights into antifungal–target interactions and may support rational drug repositioning or combination strategies.

Funding

This work was supported and funded by the Deanship of Scientific Research at Imam Mohammad Ibn Saud Islamic University (IMSIU) (grant number IMSIU-DDRSP2601)

REFERENCES CITED

Al-Rajhi, A. M. H., Qanash, H., Almashjary, M. N., Hazzazi, M. S., Felemban, H. R., and Abdelghany, T. M. (2023). "Anti-*Helicobacter pylori*, antioxidant, antidiabetic, and anti-Alzheimer's activities of laurel leaf extract treated by moist heat and molecular docking of its flavonoid constituent, naringenin, against acetylcholinesterase and butyrylcholinesterase," *Life* 13(7), article 1512. https://doi.org/10.3390/life13071512

Al-Rajhi, A. M. H., Alsalamah, S. A., Qanash, H., Bazaid, A. S., Aldarhami, A., Felemban, H. R., Gattan, H. S., AlZamil, N. M., Daws, D., and Abdelghany, T. M. (2025). "Biochemical description of ozonized propolis and its activity against pathogenic microorganisms, cancer cells, and inflammation with molecular docking interaction," *PLoS One* 20(9), article e0332224. https://doi.org/10.1371/journal.pone.0332224

Alsalamah, S. A., Alghonaim, M. I., Jusstaniah, M., and Abdelghany, T. M. (2023). "Anti-yeasts, antioxidant and healing properties of henna pre-treated by moist heat and molecular docking of its major constituents, chlorogenic and ellagic acids, with *Candida albicans* and *Geotrichum candidum* proteins," *Life* 13(9), article 1839. https://doi.org/10.3390/life13091839

Antachopoulos, C., Meletiadis, J., Sein, T., Roilides, E., and Walsh, T. J. (2008). "Comparative *in vitro* pharmacodynamics of caspofungin, micafungin, and anidulafungin against germinated and nongerminated *Aspergillus* conidia," *Antimicrob. Agents Chemother.* 52. https://doi.org/10.1128/aac.00699-07

Asif, T., Javed, U., Zafar, S. B., Ansari, A., Ul Qader, S. A., and Aman, A. (2020). "Bioconversion of colloidal chitin using novel chitinase from *Glutamicibacter uratoxydans* exhibiting anti-fungal potential by hydrolyzing chitin within fungal cell wall," *Waste and Biomass Valorization* 11(8), 4129-4143. https://doi.org/10.1007/s12649-019-00746-2

Brain, L., Bleackley, M., Doblin, M. S., and Anderson, M. (2025). "Fungal chitin synthases: Structure, function, and regulation," *J. Fungi* 11(796), https://doi.org/10.3390/jof11110796

Cedeño-Pinargote, A. C., Jara-Medina, N. R., Pineda-Cabrera, C. C., Cueva, D. F., Erazo-Garcia, M. P., Tejera, E., and Machado, A. (2025). "Impact of biofilm formation by vaginal *Candida albicans* and *Candida glabrata* isolates and their antifungal resistance: A comprehensive study in Ecuadorian women," *J. Fungi* 11(620), https://doi.org/10.3390/jof11090620

Chang, T. H., Cardona Gloria, Y., Hellmann, M. J., Richardo, T., Greve, C. L., Le Roy, D., and Weber, A. N. (2025). "Transkingdom mechanism of MAMP generation by chitotriosidase feeds oligomeric chitin from fungal pathogens and allergens into TLR2-mediated innate immune sensing," *Frontiers in immunology* 16, article 1497174. https://doi: 10.3389/fimmu.2025.1497174

Chen, G. C., and Johnson, B. R. (1983). "Improved colorimetric determination of cell wall chitin in wood decay fungi," *Applied and Environmental Microbiology* 46(1), 13-16. https://doi.org/10.1128/aem.46.1.13-16.1983

Davis, M. R., Donnelley, M. A., and Thompson III, G. R. (2020). "Ibrexafungerp: A novel oral glucan synthase inhibitor," *Med. Mycol.* 58(5), 579-592. https://doi.org/10.1093/mmy/myz083

El Ayoubi, L.W., Allaw, F., Moussa, E., and Kanj, S. S. (2024). "Ibrexafungerp: A narrative overview," *Curr. Res. Microb. Sci.* 6, article 100245. https://doi.org/10.1016/j.crmicr.2024.100245

Fuentefria, A. M., Pippi, B., Dalla Lana, D.F., Donato, K. K., and de Andrade, S. F. (2018). "Antifungals discovery: An insight into new strategies to combat antifungal resistance," *Lett. Appl. Microbiol.* 66(1), 2-13. https://doi.org/10.1111/lam.12820

Guerriero, G., Avino, M., Zhou, Q., Fugelstad, J., Clergeot, P. H., and Bulone, V. (2010). "Chitin synthases from *Saprolegnia* are involved in tip growth and represent a potential target for anti-oomycete drugs," *PLoS pathogens* 6(8), article e1001070. https://doi:10.1371/journal.ppat.1001070

Kovács, R., Nagy, F., Tóth, Z., Bozó, A., Balázs, B., and Majoros, L. (2019). "Synergistic effect of nikkomycin Z with caspofungin and micafungin against *Candida albicans* and *Candida parapsilosis* biofilms," *Lett. Appl. Microbiol.* 69(4), 271-278. https://doi.org/10.1111/lam.13204

Liu, Y., Li, R., Zhang, Y., Zong, Y., Zhang, M., Bi, Y., and Li, Y. (2026). "Chitin deacetylases AaCDAs enable *Alternaria alternata* to evade host immune responses *via* cell wall modification," *Mycology* 2647504. https://doi.org/10.1080/21501203.2026.2647504

Moussian, B. (2019). "Chitin: structure, chemistry and biology," in: *Targeting Chitin-containing Organisms, Advances in Experimental Medicine and Biology*, Q. Yang and T. Fukamizo (eds.), Vol. 1142. Springer, Singapore. https://doi.org/10.1007/978-981-13-7318-3_2

Qanash, H., Alotaibi, K., Aldarhami, A., Bazaid, A. S., Ganash, M., Saeedi, N. H., and Ghany, T. A. (2023). "Effectiveness of oil-based nanoemulsions with molecular docking of its antimicrobial potential," *BioResources* 18(1), 1554-1576. https://doi.org/10.15376/biores.18.1.1554-1576

Qanash, H., Al-Rajhi, A. M., Almashjary, M. N., Basabrain, A. A., Hazzazi, M. S., and Abdelghany, T. M. (2023). "Inhibitory potential of rutin and rutin nano-crystals against Helicobacter pylori, colon cancer, hemolysis and Butyrylcholinesterase in vitro and in silico," *Applied Biological Chemistry* 66(1), 79. https://doi.org/10.1186/s13765-023-00832-z

Santos, A. L., Rodrigues, C. F., Roudbary, M., and Branquinha, M. H. (2025). "Past, present and future of antifungals: Advancements in mechanisms of action and resistance," *Curr. Res. Microb. Sci.* 9, article 100473. https://doi.org/10.1016/j.crmicr.2025.100473

Steinbach, W. J., Cramer Jr, R. A., Perfect, B. Z., Asfaw, Y. G., Sauer, T. C., Najvar, L. K., and Perfect, J. R. (2006). "Calcineurin controls growth, morphology, and pathogenicity in *Aspergillus fumigatus*," *Eukaryot. Cell* 5(7), 1091-1103. https://doi.org/10.1128/ec.00139-06

Walker, L. A., Lee, K. K., Munro, C. A., and Gow, N. A. (2015). "Caspofungin treatment of *Aspergillus fumigatus* results in ChsG-dependent upregulation of chitin synthesis and the formation of chitin-rich microcolonies," *Antimicrob. Agents Chemother.* 59(10), 5932-5941. https://doi.org/10.1128/AAC.00862-15

Walker, L. A., Munro, C. A., de Bruijn, I., Lenardon, M. D., McKinnon, A., and Gow, N. A. (2008). "Stimulation of chitin synthesis rescues *Candida albicans* from echinocandins," *PLoS Pathog.* 4, article e1000040. https://doi.org/10.1371/journal.ppat.1000040

Xu, H., Li, Y., Cao, X., He, Q., Jin, B., Dai, L., and Hang, L. (2025). "Discovery of novel inhibitors targeting fungal chitin deacetylase *via* virtual screening for plant disease control," *Journal of Agricultural and Food Chemistry* 73(15), 8886-8896. https://doi.org/10.1021/acs.jafc.5c00847

Yahya, R., Al-Rajhi, A. M. H., Alzaid, S. Z., Al Abboud, M. A., Almuhayawi, M. S., Al Jaouni, S. K., Selim, S., Ismail, K. S., and Abdelghany, T. M. (2022). "Molecular docking and efficacy of *Aloe vera* gel based on chitosan nanoparticles against *Helicobacter pylori* and its antioxidant and anti-Inflammatory activities," *Polymers* 14, article 2994. https://doi.org/10.3390/polym1415299

Article submitted: February 22, 2026; Peer review completed: May 11, 2026; Revised version received: May 13, 2026; Accepted: May 28, 2026; Published: June 23, 2026.
DOI: 10.15376/biores.21.3.7317-7330